# SIRT1 positively regulates autophagy and mitochondria function in embryonic stem cells under oxidative stress

**Xuan Ou**[*], **Man Ryul Lee**[*], **Xinxin Huang**, **Steven Messina-Graham**, and **Hal E. Broxmeyer**[**]

Department of Microbiology and Immunology, Indiana University School of Medicine, Indianapolis, Indiana, USA

## Abstract

SIRT1, an NAD-dependent deacetylase, plays a role in regulation of autophagy. SIRT1 increases mitochondrial function and reduces oxidative stress, and has been linked to age-related reactive oxygen species (ROS) generation, which is highly dependent on mitochondrial metabolism. $H_2O_2$ induces oxidative stress and autophagic cell death through interference with Beclin 1 and the mTOR signaling pathways. We evaluated connections between SIRT1 activity and induction of autophagy in murine (m) and human (h) embryonic stem cells (ESCs) upon ROS challenge. Exogenous $H_2O_2$ (1mM) induced apoptosis and autophagy in wild-type (WT) and *Sirt1−/−* mESCs. High concentrations of $H_2O_2$ (1mM) induced more apoptosis in *Sirt1−/−*, than in WT mESCs. However, addition of 3-Methyladenine (3-MA), a widely used autophagy inhibitor, in combination with $H_2O_2$ induced more cell death in WT than in *Sirt1−/−* mESCs. Decreased induction of autophagy in *Sirt1−/−* mESCs was demonstrated by decreased conversion of LC3-I to LC3-II, lowered expression of Beclin-1, decreased LC3 punctae and LysoTracker staining. $H_2O_2$ induced autophagy with loss of mitochondrial membrane potential and disruption of mitochondrial dynamics in *Sirt1−/−* mESCs. Increased phosphorylation of P70/85-S6 kinase and ribosomal S6 was noted in *Sirt1−/−* mESCs, suggesting that SIRT1 regulates the mTOR pathway. Consistent with effects in mESCs, inhibition of *SIRT1* using Lentivirus-mediated *SIRT1 shRNA* in hESCs demonstrated that knock-down of *SIRT1* decreased $H_2O_2$-induced autophagy. This suggests a role for SIRT1 in regulating autophagy and mitochondria function in ESCs upon oxidative stress, effects mediated at least in part by the class III PI3K/Beclin 1 and mTOR pathways.

[**]Correspondence to: Hal E. Broxmeyer, PhD, Department of Microbiology and Immunology, Indiana University School of Medicine, 950 West Walnut Street, Indianapolis, IN 46202-5181 USA, Phone: 317-274-7510, Fax: 317-274-7592, hbroxmey@iupui.edu.
[*]These authors contributed equally to this work.

**Author Contributions:**

Xuan Ou: Conception and design, Collection and/or assembly of data, Data analysis and interpretation, Manuscript writing
Man Ryul Lee: Collection and/or assembly of data, Data analysis and interpretation, Manuscript Writing
Xinxin Huang: Collection and/or assembly of data and Manuscript Writing
Steven Messina-Graham: Data analysis and interpretation
Hal E. Broxmeyer: Conception and design, Financial support, Manuscript writing, and Final approval of manuscript.

**Disclosure of potential conflicts of interest**

Hal E. Broxmeyer is a member of the Medical Scientific Advisory Board of Corduse, a cord blood banking company based in Orlando, Florida.

## Introduction

Autophagy is a stress-induced catabolic process involving intracellular degradation and recycling of cytoplasmic materials through lysosomal machinery [1]. During autophagy, cytoplasmic materials, such as protein aggregates and organelles, are sequestered within a double-membrane vesicle named the autophagosome. The autophagosomes then fuse with lysosomes to form autolysosomes, which leads to degradation of cellular structures and subsequent recycling of nutrients and membranes [2]. Autophagy has often been regarded as a defense mechanism to protect cells under stress conditions, such as starvation. However, excessive autophagy results in autophagic cell death referred to as type II programmed cell death (PCD), which is distinct from type I PCD (apoptosis) and necrosis [2]. Autophagy plays a pivotal role in anticancer, antiaging, antimicrobial defense, neuroprotection, and development [3].

The mammalian silent information regulator 2 homolog, SIRT1, is an NAD-dependent histone deacetylase that plays a major role in regulating gene expression, metabolism, cancer, aging and development [4–6]. SIRT1 regulates several transcription factors such as FOXO, tumor suppressor p53, and nuclear factor-kappa B (NF-$\kappa$B) [4]. SIRT1 modulates key target proteins to maintain mitochondrial function, including peroxisome proliferator-activated receptor gamma coactivator (PGC)-1$\alpha$, adenosine monophosphate-activated protein kinase, and FOXO3a [7–9]. SIRT1 regulates the autophagy-lysosome pathway by deacetylation of autophagy-related genes Atg5, Atg7, Atg8, and FoxO1 [10, 11]. A SIRT1 activator, resveratrol, also has been shown to induce autophagic cell death in chronic myelogenous leukemia cells through JNK-mediated p62 expression and AMPK activation [12]. However, the influence of the SIRT1/autophagy pathway on mitochondrial function in ESCs has not yet been elucidated.

Cellular oxidative stress and increased reactive oxygen species (ROS) generation induces autophagy under conditions of starvation, ischemia/reperfusion or, hypoxia [13]. A ROS-generating agent, $H_2O_2$, induces oxidative stress and autophagic cell death through interference with Beclin 1 and Akt/mTOR signaling pathways in cancer cells [14, 15]. Two SIRT1 activators, resveratrol and SRTAW04, reduce oxidative stress and regulate mitochondrial function in neuronal cells by activation of SIRT1 [16].

Our previous studies [6, 17] showed that low concentrations of exogenous $H_2O_2$ (0.2–0.4mM) induced more apoptosis in wild-type (WT) than in *Sirt1–/–* mESCs. In contrast, higher concentrations of $H_2O_2$ (1mM) induced more apoptosis and higher expression of BAX and PUMA in *Sirt1–/–* than WT mESCs, suggesting that SIRT1 participates in protecting cells upon challenge at relatively high ROS concentrations (0.5mM–1mM $H_2O_2$). Based on the likely activation of autophagy under starved conditions and that SIRT1 is an important *in vivo* regulator of autophagy [10], we evaluated connections between SIRT1 activity and induction of autophagy in ESCs upon ROS challenge.

## Materials and Methods

### mESC culture

Mouse ES cell line R1 and *Sirt1−/−* mESCs derived from R1 parental cells (A kind gift from Dr. McBurney, Ottawa, Canada) were cultured as reported [18] on irradiated mouse embryonic fibroblasts in Dulbecco modified Eagle medium with 15% fetal bovine serum (FBS) (Hyclone Laboratories, Logan, UT), 1000 U/mL LIF (Chemicon International, Temecula, CA), 100U/mL penicillin/streptomycin (Invitrogen, Corp., Carlsbad, CA, http://www.invitrogen.com/), L-Glutamine 200 mM (100 ×) (Gibco, Carlsbad, CA), 0.1 mM nonessential amino acids (Invitrogen, Carlsbad, CA), and 0.1 mM β-mercaptoethanol (Invitrogen, Carlsbad, CA) at 37°C/5% CO2. Media was changed daily, and cells were passaged every 2 to 3 days.

### hESC culture

The hESC H9 cell line was used according to the research protocol of the WiCell Research Institute (WiCell, Madison, WI, http://www.wicell.org). These cells were plated as colonies and cultured on a feeder layer of mouse embryonic fibroblasts (MEFs) inactivated with 10μg/ml mitomycin C (Sigma-Aldrich, St. Louis, CA, http://www.sigmaaldrich.com) and seeded at $2 \times 10^5$ cells per 35-mm dish at 5% $CO_2$ and with a daily change of Dulbecco's modified Eagle's medium (DMEM)/F12, containing 20% serum replacement, 1 mM glutamine, 0.1% nonessential amino acids, 0.1% penicillin/streptomycin, 0.1 mM beta-mercaptoethanol, and 4 ng/ml recombinant human FGF-2 (Invitrogen, Corp., Carlsbad, CA). For passaging, hESC colonies were mechanically detached with a glass pipette during transfer. Passages were made at a 1:2 or 1:3 split ratio [19]. For transduction of *SIRT1* shRNA and $H_2O_2$ treatment, hESCs were cultured in mTeSR1 medium (STEMCELL Technologies Vancouver, Canada, http://www.stemcell.com/) on matrigel-coated dishes, as described in the manufacturer's protocol.

### Treatment with inhibitors and Annexin V apoptosis detection assay

WT and SIRT1−/− mESCs were pretreated with 3-MA (10 mM), Z-VAD-FMK (25 μM), or Bafilomycin (1 nM) which were purchased from Sigma-Aldrich (St. Louis, CA, http://www.sigmaaldrich.com) for half an hour. The cells were treated with $H_2O_2$ (0.6 mM or 1mM) for 4 hours with the same media used for control maintaining experiments. The experiments were completed after the 4-hour treatment with $H_2O_2$. After treatment, Annexin V apoptosis detection assay was performed following the manufacture's instruction (BD Biosciences, San Jose, CA, http://www.bdbiosciences.com/). Briefly, Annexin V (FITC labeled, 5μL), propidium iodide (5μL), and the binding buffer (400μL), were added to a final volume of 500μL, analysis was performed within an hour by FACScan flow cytometry.

### Measurement of caspase activity

Caspase activity was measured using an active caspase-3 antibody (BD Biosciences, San Jose, CA, http://www.bdbiosciences.com). In brief, cells were washed once in PBS, then fixed and permeabilized using the Cytofix/Cytoperm (BD Biosciences) for 20 min at room temperature, pelleted and washed with Perm/Wash™ buffer (BD Bioscience). Cells were

subsequently stained with the FITC rabbit anti-active caspase-3 antibody (BD Bioscience). Cells were then washed and resuspended in BD Perm/Wash™ buffer before analysis by flow cytometry.

### Measurement of intracellular ROS

After experimental treatments, cells were washed 3× with PBS. Cells were then incubated with 10μg/ml dichlorofluorescein diacetate (DCF-DA) (Sigma-Aldrich, St. Louis, MO) for 20 min at 37°C [17]. Then cells were washed twice in phosphate-buffered saline (PBS), trysinized, washed in PBS and then DCF-DA fluorescence was measured with a FACScan flow cytometry (BD Biosciences, San Jose, CA). Data were analyzed with FlowJo software (Tree Star, Inc., Ashland, OR, http://www.treestar.com/) and mean fluorescence intensity was quantitated.

### Measurement of mitochondrial membrane potential

WT and SIRT1−/− mESCs were pretreated with 3-MA (10 mM) for half an hour, then cells were treated with 1 mM $H_2O_2$ for 4 hours with the same media used for control experiments. The experiments were completed by washing the cells 3× with PBS after the 4-hour treatment with $H_2O_2$. After $H_2O_2$ treatment, mitochondrial membrane potential was measured using the MitoProbe™ JC-1 Assay Kit for Flow Cytometry (Invitrogen, Corp., Carlsbad, CA, http://www.invitrogen.com/) performed following the manufacturer's instructions.

### Immunocytochemistry

Cells were fixed in 4% paraformaldehyde for 20 min at room temperature and permeabilized with 0.2% Triton X-100 containing 1% bovine serum albumin (BSA) in phosphate-buffered saline (PBS) for 15 minutes. After blocking with 1% BSA, fixed cells were incubated overnight at 4°C with primary antibodies against LC3 (1:100 dilution; Cell Signaling, Danvers, MA, http://www.cellsignal.com/) or lysosomal-associated membrane protein-1 (LAMP-1, 1:200 dilution; Hybridoma Bank, Iowa City, IA, http://dshb.biology.uiowa.edu/). Stained cells were washed and incubated for 2 hours at room temperature with AlexaFluor-conjugated secondary antibodies (AlexaFluor 555-donkey anti–mouse IgG 1:500 dilution or AlexaFluor 488-donkey anti–rabbit IgG 1:500 dilution; Molecular Probes, http://www.invitrogen.com/). After incubation with secondary antibodies, cells were stained with nuclear dye DAPI (Life technologies, Grand Island, NY, www.lifetechnologies.com/) in PBS for 5 minutes at room temperature. For negative controls, cultured cells were incubated with secondary antibody only.

### Western blot analysis

After washing with serum-free medium, ESCs were suspended in lysis buffer (Thermo Scientific) and centrifuged. Equal amounts of proteins were separated by SDS-PAGE on 10% polyacrylamide gels and transferred to polyvinylidene difluoride membranes (Millipore, Billerica, MA, http://www.millipore.com). The membranes were blocked with 5% nonfat dried milk for 1 hour and incubated overnight at 4°C with anti-LC3 (1:1000 dilution), anti–beclin-1, anti–cleaved caspase-3 (1:1000 dilution), anti-bax (1:1000 dilution),

ribosomal S6 (1:1000 dilution), phospho-ribosomal S6 (ser235/236), phosphor-p70 S6 kinase (T389) or anti-ATG-7 (1:1000 dilution) followed by incubation with horseradish peroxidase-conjugated goat anti–rabbit IgG (1:10,000 dilution) which were purchased from Cell Signaling company with anti-β-actin (1:5,000 dilution; Sigma, St. Louis, MO) antibody followed by incubation with horseradish peroxidase-conjugated goat anti–mouse IgG (1:10,000 dilution; Cell Signaling, Danvers, MA). For SIRT1immunoblotting, treatment with anti–SIRT1 (1:500; Santa Cruz Biotechnology Inc., Santa Cruz, CA, http://www.scbt.com) antibody was followed by treatment with horseradish peroxidase-conjugated goat anti–mouse IgG (1:10,000 dilution; Pierce). Immunoreactive proteins were visualized using a chemiluminescence substrate (Millipore, Billerica, MA) and quantitatively analyzed by densitometry using ImageJ software (developed by Wayne Rasband, National Institutes of Health, Bethesda, MD). All experiments were performed in triplicate.

### SIRT1 inhibition with shRNA

*SIRT1* specific shRNA and control shRNA were Silencer select pre-designed shRNAs purchased from Santa Cruz (Santa Cruz Biotechnology Inc., Santa Cruz, CA, http://www.scbt.com), and experiments were performed according to manufacturer's instructions. Briefly, hESCs were seeded on Matrigel-coated dishes 1 day before transduction. On the day of transduction, culture medium was replaced by virus-containing supernatant supplemented with 8 ug/ml polybrene and incubated overnight. Cells were treated 24 hours later with $H_2O_2$ with or without 3-MA treatment, and cell pellet was collected.

### Statistical analysis

All data are presented as mean ± SD. Statistical Analysis Testing was performed using Prism 5 graph pad (http://www.graphpad.com/scientific-software/prism/) software. Statistical significance (A P-value <0.05 was considered statistically significant) was calculated using Student t test in cases of two comparison groups and one-way analysis of variance (ANOVA) with Tukeys correction in cases of more than two comparison groups

## Results

### $H_2O_2$ induced cell death in WT and *Sirt1–/–* mESCs

Effects of exogenous $H_2O_2$ on apoptosis in WT and *Sirt1–/–* mESCs were analyzed (Figure 1). Consistent with our previous reports [5, 6, 17], higher concentrations of $H_2O_2$ (1mM) induced more apoptosis in *Sirt1–/–* than in WT mESCs. To evaluate whether autophagy is induced in WT and *Sirt1–/–* mESCs after treatment with exogenous $H_2O_2$, 3-Methyladenine (3-MA), a widely used autophagy inhibitor [12], was employed. Cells were treated with $H_2O_2$ in the presence or absence of 3-MA. In WT cells, $H_2O_2$-induced apoptosis was increased by the addition of 3-MA. In contrast, apoptosis was not affected by the addition of 3-MA to *Sirt1–/–* mESCs. 3-MA alone had no effect on cell viability (Figure 1A). Cell-permeable pan-caspase inhibitor z-VAD-FMK (25μM) was used to evaluate caspase-dependent apoptosis. However, z-VAD-FMK did not decrease the cell viability compared with $H_2O_2$-treated cells (Figure 1A). Next, we analyzed caspase 3 activity. Both WT and *Sirt1–/–* $H_2O_2$-treated cells demonstrated increased caspase-3 activity compared to the control group, but there was a greater degree of activation of caspase-3 in *Sirt1–/–*

$H_2O_2$-treated cells than in $H_2O_2$-treated WT cells (Figure 1B). While there is no effect on caspase-3 activation in the *Sirt1−/−* $H_2O_2$-treated group in the presence of 3-MA, there is increased activated caspase-3 in $H_2O_2$-treated WT cells above that of 3-MA treatment (Figure 1B), which is consistent with results of the Annexin-V apoptosis detection assay (Figure 1A). To evaluate whether there is a difference between WT and *Sirt1−/−* mESCs treated with lower concentrations of $H_2O_2$, apoptosis was evaluated in R1 and *Sirt1−/−* mESCs treated with 0.6 mM $H_2O_2$ in the presence or absence of 3-MA (Figure 1C). The addition of 3-MA to $H_2O_2$ did not significantly induce differences in apoptosis between WT and *Sirt1−/−* mESCs (Figure 1C). Therefore, 1mM $H_2O_2$ was used to evaluate autophagy induction in control and *Sirt1−/−* mESCs.

### *Sirt1−/−* mESCs are less sensitive than WT cells to $H_2O_2$ induction of autophagy

We evaluated whether $H_2O_2$-induced autophagy was stimulated in control and *Sirt1−/−* mESCs (Figure 2). To measure autophagy after $H_2O_2$ treatment, the widely used autophagosome marker LC3, the mammalian homolog of Atg8, was measured. WT cells treated with $H_2O_2$ for 4 hour began to show increased formation of LC3 punctae, whereas non-treated WT cells barely showed LC3 dots (Figure 2A and B). After addition of 3-MA, WT cells showed significantly reduced LC3 dots compared to $H_2O_2$–treated cells, suggesting induction of autophagy in WT cells treated with $H_2O_2$. In contrast, after treatment with $H_2O_2$, *Sirt1−/−* cells showed fewer perinuclear LC3 dots, and addition of 3-MA did not significantly affect the formation of LC3 punctae (Figure 2A and B). To further prove induction of autophagy, we performed live-cell confocal microscopy using LysoTracker, a dye for lysosomes (Figure 2C). Whereas lysosomes were small in nontreated control cells, they were greatly increased in size and staining in cells treated for 1 hour with $H_2O_2$. Consistent with reduced LC3 dots, less LysoTracker was expressed in *Sirt1−/−* cells treated with $H_2O_2$ (Figure 2C). To evaluate the final stage of autophagy, the fusion of autophagosomes with lysosomes [20, 21], we performed double immunostaining with anti-LC3 and anti-Lysosomal-associated membrane protein 1 (LAMP-1) antibodies using chloroquine (CQ). Chloroquine is an autophagic flux inhibitor, which was used to assess the turnover of LC3, which gives a relative level of autophagy. As shown in Figure 2D, both WT and *Sirt1−/−* mESCs exhibit LC3 and LAMP-1 co-localization, suggesting that SIRT1 does not affect the final step of fusion of autophagosomes with lysosomes. The above information indicates that $H_2O_2$ induces less autophagy activation in *Sirt1−/−* mESCs, compared to that induced in WT cells, but the down-stream effects of autophagy (autophagasome/lysosome fusion) are not defective. Rather the effect lies upstream in the activation of the autophagy process.

### $H_2O_2$ induces autophagy with loss of mitochondrial membrane potential and disruption of mitochondrial dynamics in *Sirt1−/−* mESCs

Accumulation of ROS in mitochondria leads to mitochondrial permeability and results in a collapse of mitochondrial membrane potential [2]. To investigate the mechanism by which $H_2O_2$ activated ROS was induced, cellular oxidative stress was estimated by monitoring generation of ROS using the fluorescence dye CM-$H_2$DCFDA. Compared to *Sirt1−/−* cells, exposure to 1mM $H_2O_2$ caused an increase of 20% in intracellular ROS accumulation in WT cells (Figure 3A and B). In WT cells, addition of CQ or 3-MA significantly increased ROS

generation by $H_2O_2$, whereas in *Sirt1–/–* mESCs, addition of CQ or 3-MA did not augment accumulation of ROS compared to $H_2O_2$ treated *Sirt1–/–* mESCs. These results suggest that SIRT1 is essential for mediating the generation of ROS by autophagy inhibition. Next, the effects of $H_2O_2$ on mitochondrial membrane potential and mitochondrial mass were evaluated (Figure 3C–E). To further determine whether $H_2O_2$ treatment results in loss of mitochondrial membrane potential, and how this is affected by SIRT1, JC-1 staining was used. WT and *Sirt1–/–* cells were treated for 4 hours with 1mM $H_2O_2$ in the presence or absence of 3-MA, and cells analyzed by flow cytometry after JC-1 staining. Mitochondrial depolarization is indicated by a decrease in the JC-1 red/green fluorescence intensity ratio. The ratio of green to red fluorescence is dependent only on the membrane potential and not on other factors. 3-MA addition alone did not affect the membrane potential in either *Sirt1–/–* or WT mESCs. After $H_2O_2$ treatment, both cell lines showed an increased fluorescence emission shift from red to green, but there was greater shifting in *Sirt1–/–* cells than in WT cells, consistent with increased apoptosis induced in *Sirt1–/–* cells. With the addition of 3-MA, there is an increased shifting in WT cells compared to the $H_2O_2$ only treatment group, while there is no difference in the *Sirt1–/–* group (Figure 3C and D). These results suggest that autophagy inhibition induces more loss of mitochondrial membrane potential after $H_2O_2$ treatment, and this is mediated by SIRT1.

Chloroquine (CQ) inhibits autophagy as it raises lysosomal pH, which leads to inhibition of fusion of autophagosome with lysosome, and lysosomal protein degradation [22]. Similar to the results of ROS generation, addition of 3-MA or CQ increased mitochondrial mass in WT cells, but not in *Sirt1–/–* cells (Figure 3E). We speculate that the increase of mitochondrial mass seen in WT cells in response to $H_2O_2$ resulted from failure of mitophagy but not from bona fide growth of mitochondria. This speculation was based on our results that the increase of mitochondria was apparent when cells were treated with chloroquine or 3-MA, inhibitors of autophagic flux which block clearance of mitochondria through mitophagy.

## $H_2O_2$ treatment increases levels of autophagy markers in WT, but not *Sirt1–/–* mESCs

Given that SIRT1 appears to be required for $H_2O_2$ stimulated autophagy, we further characterized the role of SIRT1 in regulation of autophagy-related signaling pathway by investigating the class III PI3K/Beclin 1 pathway. Autophagy associated protein LC3 is the mammalian equivalent of yeast Atg8 [15]. LC3 is post-translationally cleaved and localized in the cytosol (LC3-I) or in autophagosomal membranes (LC3-II). Thus, detection of LC3-II can be used to estimate the abundance of autophagosomes. Addition of compounds such as Bafilomycin A which blocks autophagic flux, can be used to estimate the relative rate of autophagy [23]. As shown in Figure 4A, $H_2O_2$ treatment for 4hr resulted in accumulation of LC3-II, and the conversion of LC3-I to LC3-II were significantly higher in the $H_2O_2$-treated WT cells compared to non-treated WT. $H_2O_2$ treatment failed to induce the conversion of LC3-I to LC3-II in Sirt1–/– mESCs. However, in the $H_2O_2$-treated Sirt1–/– mESCs, the LC3 conversion was significantly lower than in the $H_2O_2$-treated WT cells. Furthermore, addition of Bafilomycin A to the $H_2O_2$-treated Sirt1–/– cells revealed significantly lower autophagic flux than $H_2O_2$-treated WT cells. These results suggest that Sirt1 plays a positive role in the early events of autophagy induction. Expression of autophagy-associated protein Beclin-1 protein was unregulated by treatment with 1mM $H_2O_2$, but down-regulated by

treatment with $H_2O_2$ and 3-MA or 1 nM Bafilomycin in WT cells. However, *Sirt1 –/–* cells revealed decreased expression of Beclin-1 in the $H_2O_2$-treated group compared to $H_2O_2$-treated WT cells. Furthermore, in order to test autophagosome flux in *Sirt1 –/–* cells, we assessed the expression of p62 (SQSTM1; sequestosome 1) which is ubiquitin binding protein degraded by the autophagosome and involved in cell signaling, oxidative stress and autophagy [12]. Western blotting revealed that expression of p62 decreased to low levels in $H_2O_2$ treated WT mESCs compared to control but conversely, autophagy inhibitors stabilized p62 levels suggesting that lysosomal degradation of autophagosomes leads to a greater decrease in p62 levels in WT mESCs during autophagy. We also confirmed $H_2O_2$ induced apoptosis in both WT and Sirt1–/– mESCs. $H_2O_2$ enhanced expression of pro-apoptotic gene Bax and cleaved caspase-3 in both cell lines compared to the control groups (Figure 4B), which is consistent with results of the apoptosis detection assay shown in Figure 1A and 1B, and our previous reports [5, 6, 17].

### Decreased induction of autophagy in SIRT1-knock down hESCs

To determine a role for SIRT1 in hESC line H9, we investigated whether these cells would respond to $H_2O_2$ in a manner similar to that of mESCs after inhibition of SIRT1 expression using Lentivirus-mediated *SIRT1 shRNA* knockdown. SIRT1 was successfully suppressed in H9 hES cells upon shRNA treatment (Figure 4C). To examine the effect of $H_2O_2$ on induction of autophagy in hES cells, we assessed effects of different $H_2O_2$ concentrations. Through a titration of $H_2O_2$ on hESCs versus mESCs, we found that this hESC line was more sensitive to $H_2O_2$-induced stress than mES cells, and a concentration of 0.1mM $H_2O_2$ was used in the following experiments with hESCs. After treatment with 0.1mM $H_2O_2$ for 30 min, WT-scrable control cells showed high basal level of LC3-II, whereas addition of 3-MA resulted in decreased amounts of LC3-II. This suggests that autophagy in WT cells is induced by $H_2O_2$, whereas the addition of 3-MA reduced conversion of LC3-I to LC3-II. In contrast, $H_2O_2$ treatment failed to induce increased LC3-II in hESCs transduced with SIRT1 shRNA compared to WT control group. Expression of autophagy-associated protein Beclin-1 and ATG-7 were increased in the WT-scramble control cells by treatment with 0.1mM $H_2O_2$, but it was down-regulated by treatment with both $H_2O_2$ and 3-MA. However, with the inhibition of SIRT1 in WT cells, Beclin-1 and ATG7 were less activated after treatment with $H_2O_2$ in hESCs transduced with Lentivirus mediated SIRT1 shRNA (Figure 4C).

### $H_2O_2$ induces autophagy through the mTOR pathway in ESCs

To get more insight into mechanisms of $H_2O_2$ induced autophagy, we evaluated the mTOR pathway. mTOR, which negatively regulates autophagy, is important for autophagy processing. Previous reports have demonstrated that SIRT1 interacts with mTOR complex [24, 25], and SIRT1 negatively regulates mTOR signaling in MEFs and human Hela cells [26]. This suggested that SIRT1 might positively regulate autophagy by suppressing the mTOR pathway. To evaluate this possibility, we analyzed phosphorylation of p70/85 S6 kinase and S6 ribosomal protein, two mTOR substrates, in WT and *Sirt1 –/–* mESCs. As shown in Figure 5A, $H_2O_2$-treated WT cells showed decreased phosphorylation of p70/ S6 kinase and S6 ribosomal protein compared to the $H_2O_2$-treated Sirtl–/– cells, which is consistent with a previous report by others [12]. When autophagy was inhibited by 3-MA in

the $H_2O_2$-treated group, WT cells showed increased phosphorylation of p70/ S6 kinase and S6. In contrast, absence of SIRT1 resulted in increased phosphorylation of p70/S6 kinase and S6 after $H_2O_2$ treatment, but not in the presence of 3-MA (Figure 5A). We further investigated whether hESCs after inhibition of SIRT1 would respond to $H_2O_2$ in a manner similar to that of *Sirt1–/–* mESCs. After treatment with 0.1mM $H_2O_2$ for 30 minutes, phosphorylation of p70/85 S6 kinase and S6 were increased in hESCs transduced with Lentivirus mediated *SIRT1* shRNA compared with cells transduced with scrambled shRNA (Figure 5B). Addition of 3-MA during $H_2O_2$ treatment of SIRT1 shRNA knock down hESCs resulted in a relative decrease in phosphorylation of p70/85 S6 kinase and S6. All the above suggests that SIRT1 positively regulates autophagy at least in part by suppressing the mTOR pathway in ESCs.

To verify that SIRT1 effects on autophagy were specifically due to the knockout of SIRT1, and not to genetic drifting of these cells, *Sirt1–/–* mESCs that were reconstituted with a WT SIRT1 gene were evaluated. This cell line was created as described by us previously [5]. Vector containing an EGFP gene alone was used as a control for the SIRT1 knockin to *Sirt1–/–* mESCs. $H_2O_2$ treatment induced conversion of LC3-I to LC3-II in *Sirt1–/–* and SIRT1 reconstituted *Sirt1–/–* cells, but there was greater conversion of LC3-I to LC3-II in the SIRT1 reconstituted group. Expression of Beclin-1 was significantly increased with reconstitution of SIRT1 to a level comparable to that of WT cells after treatment with $H_2O_2$. With addition of 3-MA, Beclin-1 was down-regulated with reconstitution of SIRT1 in $H_2O_2$-treated, but not in *Sirt1–/–* cells transduced with EGPF only mESCs (Figure 5C). This verifies that decreased activation of autophagy observed in *Sirt1–/–* cells after $H_2O_2$ stress was specific to deletion of SIRT1.

## Discussion

In the current studies, we demonstrated that: (1) SIRT1 activity is necessary for oxidative stress-induced autophagy and apoptosis in mESCs and hESCs; (2) SIRT1 deficiency results in greater loss of mitochondrial membrane potential after $H_2O_2$ treatment; and (3) SIRT1 mediates oxidative stress-induced autophagy through the class III PI3K/Beclin 1 and mTOR pathways. Overall, our study reveals that SIRT1 and activation of autophagy form an essential protective mechanism for cell survival under oxidative stress conditions.

SIRT1, the best-studied Sirtuin protein family member, is involved in various physiological processes including aging, energy metabolism and stress response [4]. SIRT1 has been considered as a potential therapeutic target for several diseases, such as cancer, Alzheimer's, diabetes and atherosclerosis [27, 28]. Studies in model organisms show extended lifespan by overexpressing SIRT1 homologues in yeast, worms, flies and mice [29]. One mechanism regarding the lifespan extension capability of SIRT1 involves chromatin remodeling and deacetylation of key heterochromatin regions [30]. In response to stress, SIRT1 acts as a pro-survival molecule that is associated with phosphorylation on its conserved Thr522 residue [31].

Autophagy is a key catabolic process that allows for the recycling and degradation of proteins and organelles through lysosome machinery, which has been linked to

neurodegenerative disorders, infectious diseases, cancer and other disorders [32, 33]. Several lines of evidence support an essential role for *Sirt1* in the induction of autophagy [10, 11]. In particular, autophagy induced by SIRT1 prevents prion peptide neurotoxicity, and resveratrol, a SIRT1 agonist, has been reported to activate autophagy and reduce rotenone-mediated neurotoxicity [34, 35]. Also, resveratrol has been reported to trigger autophagic cell death in Chronic Myelogenous Leukemia cells via both AMPK and JNK activation [12]. Consistent with these reports, we found that in *Sirt1−/−* ESC there was less oxidative stress-induced autophagy as measured by the ratio of LC3-I to LC3-II, expression of Beclin1, and decreased LC3 punctae and LysoTracker staining (Figure 2 A–C & Fig 4A–C). Since autophagy is important for various cellular processes and inappropriately increased or decreased autophagy activities are associated with pathological states, cellular autophagy levels should be tightly controlled. Various signaling pathways have been reported to regulate autophagy. mTOR, which is the most studied pathway regulating autophagy, inhibits initiation of autophagy through the ULK1/2-ATG13-FIP200 complex. An interesting finding of our work (Figure 5A) is that SIRT1 deficiency results in more phosphorylation of mTOR substrates, p70/85 S6 kinase and S6, suggesting SIRT1 may regulate autophagy at upstream initiation steps in ESCs This is further supported by the evidence that both WT and *Sirt1−/−* cells exhibit LC3 and LAMP-1 co-localization, suggesting that SIRT1 does not affect the final step of fusion of autophagosomes with lysosomes (Figure 2D).

Autophagy is usually regarded as a protective process that prepares the cell to survive under various stress conditions. Autophagy deficient mice, such as Atg3, Atg5 or Atg7 knockout mice, die at birth, indicating that autophagy inhibits cell death [36]. Conversely, accumulating evidence shows that autophagy also contributes to cell death, which is referred as "autophagic cell death" [37–39]. In our case, lower concentrations of exogenous $H_2O_2$ induced more apoptosis in wild-type than in *Sirt1−/−* mESCs [17], while higher concentrations of $H_2O_2$ induced more apoptosis in *Sirt1−/−* than in wild-type mESCs. This suggests that autophagy is a protective or cell-death inhibitor under higher oxidative stress conditions. Inhibition of autophagy by 3-MA in wild type cells mirrors the higher oxidative stress-triggered cell death phenotype in *Sirt1−/−* mESCs.

Although ROS is generated during basal cellular respiration, increased levels of ROS (free radicals i.e., $O_2^-$, $HO\cdot$ or nonradicals i.e., $H_2O_2$) can oxidize cellular components and injure DNA, lipids and proteins of the cell. ROS induces autophagy by inhibition of ATG4 activity [40]. Additionally, increased ROS can induce autophagic cell death through Beclin1 and the mTOR signaling pathway [13, 41]. SIRT1 has been linked to age-related ROS, which is highly dependent on mitochondria metabolism [42]. Here, for the first time we show that SIRT1 is an important bridging molecular link between ROS and autophagy via regulation of the class III PI3K/Beclin 1 and mTOR pathways. Mitochondria are main targets of oxidative stress and loss of mitochondrial membrane potential and mitochondrial impairment have been linked with autophagy [43, 44]. In our work, we demonstrated activated autophagy and collapse of mitochondrial membrane potential after $H_2O_2$ treatment of ESCs, while an even more severe mitochondrial phenotype was observed in *Sirt1−/−*

mESCs, suggesting that SIRT1 triggered autophagy is involved in the maintenance of mitochondrial function and thus, protection of cells (Figure 3A–E).

As repeated by others, SIRT1 is involved in the induction of autophagy and protects neuronal cells, cardiomyocytes and embryonic fibroblasts [10, 11, 34]. Consistently, we reveal that SIRT1 is also essential for oxidative stress-induced autophagy that in turn affects cell survival in mESCs and hESCs. Thus, function of SIRT1 appears to be conserved in both somatic cells and ESCs. SIRT1 also plays important roles in the differentiation of mESCs, hematopoietic stem cells and mesenchymal stem cells [5, 45]. It would be interesting to know whether this is also related to the function of SIRT1 in autophagy regulation.

## Conclusions

In summary, we have shown that regulation of autophagy by SIRT1 plays a role in ESC survival against oxidative stress induced by high concentrations of $H_2O_2$. Notably, SIRT1-mediated oxidative stress-induced autophagy results in decreased mitochondrial damage that in turn leads to less apoptosis and increased cell protection.

## Acknowledgments

## References

1. Rubinsztein DC, Codogno P, Levine B. Autophagy modulation as a potential therapeutic target for diverse diseases. Nat Rev Drug Discov. 2012; 11:709–730. [PubMed: 22935804]

2. Chen Y, Klionsky DJ. The regulation of autophagy - unanswered questions. J Cell Sci. 2011; 124:161–170. [PubMed: 21187343]

3. Focusing on autophagy. Nat Cell Biol. 2010; 12:813. [PubMed: 20811352]

4. Haigis MC, Sinclair DA. Mammalian sirtuins: biological insights and disease relevance. Annu Rev Pathol. 2010; 5:253–295. [PubMed: 20078221]

5. Ou X, Chae HD, Wang RH, et al. SIRT1 deficiency compromises mouse embryonic stem cell hematopoietic differentiation, and embryonic and adult hematopoiesis in the mouse. Blood. 2011; 117:440–450. [PubMed: 20966168]

6. Chae HD, Broxmeyer HE. SIRT1 deficiency downregulates PTEN/JNK/FOXO1 pathway to block reactive oxygen species-induced apoptosis in mouse embryonic stem cells. Stem Cells Dev. 2011; 20:1277–1285. [PubMed: 21083429]

7. Canto C, Gerhart-Hines Z, Feige JN, et al. AMPK regulates energy expenditure by modulating NAD + metabolism and SIRT1 activity. Nature. 2009; 458:1056–1060. [PubMed: 19262508]

8. Gerhart-Hines Z, Rodgers JT, Bare O, et al. Metabolic control of muscle mitochondrial function and fatty acid oxidation through SIRT1/PGC-1alpha. Embo J. 2007; 26:1913–1923. [PubMed: 17347648]

9. Kume S, Uzu T, Horiike K, et al. Calorie restriction enhances cell adaptation to hypoxia through Sirt1-dependent mitochondrial autophagy in mouse aged kidney. J Clin Invest. 2010; 120:1043–1055. [PubMed: 20335657]

10. Lee IH, Cao L, Mostoslavsky R, et al. A role for the NAD-dependent deacetylase Sirt1 in the regulation of autophagy. Proc Natl Acad Sci U S A. 2008; 105:3374–3379. [PubMed: 18296641]

11. Hariharan N, Maejima Y, Nakae J, et al. Deacetylation of FoxO by Sirt1 Plays an Essential Role in Mediating Starvation-Induced Autophagy in Cardiac Myocytes. Circ Res. 2010; 107:1470–1482. [PubMed: 20947830]

12. Puissant A, Robert G, Fenouille N, et al. Resveratrol promotes autophagic cell death in chronic myelogenous leukemia cells via JNK-mediated p62/SQSTM1 expression and AMPK activation. Cancer Res. 2010; 70:1042–1052. [PubMed: 20103647]

13. Essick EE, Sam F. Oxidative stress and autophagy in cardiac disease, neurological disorders, aging and cancer. Oxid Med Cell Longev. 2010; 3:168–177. [PubMed: 20716941]

14. Chen Y, McMillan-Ward E, Kong J, et al. Oxidative stress induces autophagic cell death independent of apoptosis in transformed and cancer cells. Cell Death Differ. 2008; 15:171–182. [PubMed: 17917680]

15. Zhang H, Kong X, Kang J, et al. Oxidative stress induces parallel autophagy and mitochondria dysfunction in human glioma U251 cells. Toxicol Sci. 2009; 110:376–388. [PubMed: 19451193]

16. Khan RS, Fonseca-Kelly Z, Callinan C, et al. SIRT1 activating compounds reduce oxidative stress and prevent cell death in neuronal cells. Front Cell Neurosci. 2012; 6:63. [PubMed: 23293585]

17. Han MK, Song EK, Guo Y, et al. SIRT1 regulates apoptosis and Nanog expression in mouse embryonic stem cells by controlling p53 subcellular localization. Cell Stem Cell. 2008; 2:241–251. [PubMed: 18371449]

18. Kyba M, Perlingeiro RC, Daley GQ. HoxB4 confers definitive lymphoid-myeloid engraftment potential on embryonic stem cell and yolk sac hematopoietic progenitors. Cell. 2002; 109:29–37. [PubMed: 11955444]

19. Lee MR, Kim JS, Kim KS. miR-124a is important for migratory cell fate transition during gastrulation of human embryonic stem cells. Stem Cells. 2010; 28:1550–1559. [PubMed: 20665740]

20. Bains M, Heidenreich KA. Live-cell imaging of autophagy induction and autophagosome-lysosome fusion in primary cultured neurons. Methods Enzymol. 2009; 453:145–158. [PubMed: 19216905]

21. Yoon YH, Cho KS, Hwang JJ, et al. Induction of lysosomal dilatation, arrested autophagy, and cell death by chloroquine in cultured ARPE-19 cells. Invest Ophthalmol Vis Sci. 2010; 51:6030–6037. [PubMed: 20574031]

22. Shintani T, Klionsky DJ. Autophagy in health and disease: a double-edged sword. Science. 2004; 306:990–995. [PubMed: 15528435]

23. Gonzalez-Polo RA, Niso-Santano M, Ortiz-Ortiz MA, et al. Inhibition of paraquat-induced autophagy accelerates the apoptotic cell death in neuroblastoma SH-SY5Y cells. Toxicol Sci. 2007; 97:448–458. [PubMed: 17341480]

24. Jeong H, Cohen DE, Cui L, et al. Sirt1 mediates neuroprotection from mutant huntingtin by activation of the TORC1 and CREB transcriptional pathway. Nat Med. 2012; 18:159–165. [PubMed: 22179316]

25. Wang RH, Kim HS, Xiao C, et al. Hepatic Sirt1 deficiency in mice impairs mTorc2/Akt signaling and results in hyperglycemia, oxidative damage, and insulin resistance. J Clin Invest. 2011; 121:4477–4490. [PubMed: 21965330]

26. Ghosh HS, McBurney M, Robbins PD. SIRT1 negatively regulates the mammalian target of rapamycin. PLoS One. 2010; 5:e9199. [PubMed: 20169165]

27. Taylor DM, Maxwell MM, Luthi-Carter R, et al. Biological and potential therapeutic roles of sirtuin deacetylases. Cell Mol Life Sci. 2008; 65:4000–4018. [PubMed: 18820996]

28. Milne JC, Lambert PD, Schenk S, et al. Small molecule activators of SIRT1 as therapeutics for the treatment of type 2 diabetes. Nature. 2007; 450:712–716. [PubMed: 18046409]

29. Mantel C, Broxmeyer HE. Sirtuin 1, stem cells, aging, and stem cell aging. Curr Opin Hematol. 2008; 15:326–331. [PubMed: 18536570]

30. Guarente L. Diverse and dynamic functions of the Sir silencing complex. Nat Genet. 1999; 23:281–285. [PubMed: 10545947]

31. Guo X, Williams JG, Schug TT, et al. DYRK1A and DYRK3 promote cell survival through phosphorylation and activation of SIRT1. J Biol Chem. 2010; 285:13223–13232. [PubMed: 20167603]

32. Levine B, Kroemer G. Autophagy in the pathogenesis of disease. Cell. 2008; 132:27–42. [PubMed: 18191218]

33. Choi AM, Ryter SW, Levine B. Autophagy in human health and disease. N Engl J Med. 2013; 368:651–662. [PubMed: 23406030]

34. Jeong JK, Moon MH, Bae BC, et al. Autophagy induced by resveratrol prevents human prion protein-mediated neurotoxicity. Neurosci Res. 2012; 73:99–105. [PubMed: 22465415]

35. Wu Y, Li X, Zhu JX, et al. Resveratrol-activated AMPK/SIRT1/autophagy in cellular models of Parkinson's disease. Neurosignals. 2011; 19:163–174. [PubMed: 21778691]

36. Kuma A, Mizushima N. Physiological role of autophagy as an intracellular recycling system: with an emphasis on nutrient metabolism. Semin Cell Dev Biol. 2010; 21:683–690. [PubMed: 20223289]

37. Martin DN, Baehrecke EH. Caspases function in autophagic programmed cell death in Drosophila. Development. 2004; 131:275–284. [PubMed: 14668412]

38. Espert L, Denizot M, Grimaldi M, et al. Autophagy is involved in T cell death after binding of HIV-1 envelope proteins to CXCR4. J Clin Invest. 2006; 116:2161–2172. [PubMed: 16886061]

39. Crighton D, Wilkinson S, O'Prey J, et al. DRAM, a p53-induced modulator of autophagy, is critical for apoptosis. Cell. 2006; 126:121–134. [PubMed: 16839881]

40. Scherz-Shouval R, Shvets E, Fass E, et al. Reactive oxygen species are essential for autophagy and specifically regulate the activity of Atg4. Embo J. 2007; 26:1749–1760. [PubMed: 17347651]

41. Chen SY, Chiu LY, Maa MC, et al. zVAD-induced autophagic cell death requires c-Src-dependent ERK and JNK activation and reactive oxygen species generation. Autophagy. 2011; 7:217–228. [PubMed: 21127402]

42. Mantel CR, Wang RH, Deng C, et al. Sirt1, notch and stem cell "age asymmetry". Cell Cycle. 2008; 7:2821–2825. [PubMed: 18797187]

43. Itoh T, Ito Y, Ohguchi K, et al. Eupalinin A isolated from Eupatorium chinense L. induces autophagocytosis in human leukemia HL60 cells. Bioorg Med Chem. 2008; 16:721–731. [PubMed: 17980607]

44. Lee J, Giordano S, Zhang J. Autophagy, mitochondria and oxidative stress: cross-talk and redox signalling. Biochem J. 2012; 441:523–540. [PubMed: 22187934]

45. Simic P, Zainabadi K, Bell E, et al. SIRT1 regulates differentiation of mesenchymal stem cells by deacetylating β-catenin. EMBO Mol Med. 2013:430–440. [PubMed: 23364955]
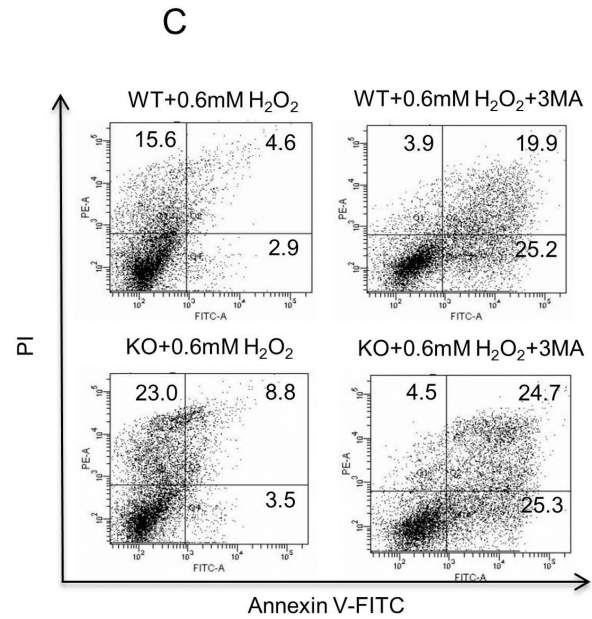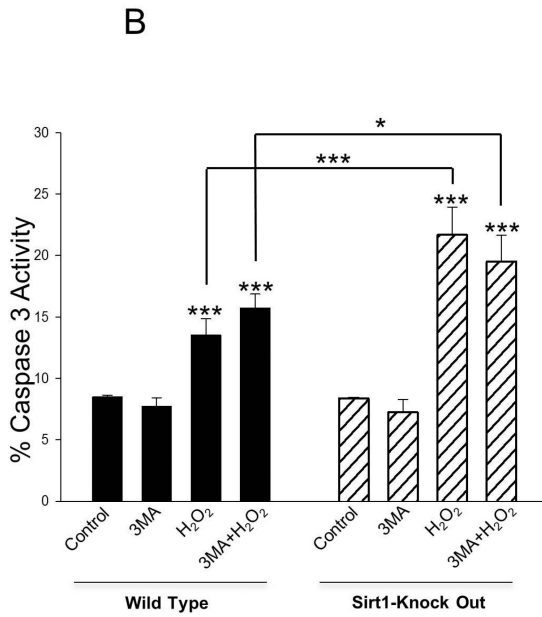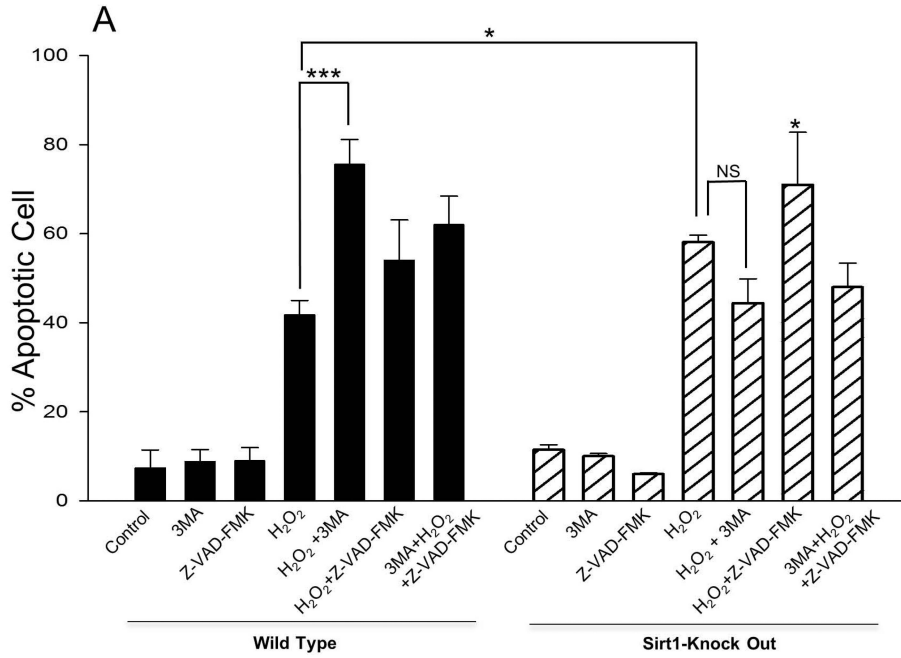
**Fig 1. 3-MA augments 1mM $H_2O_2$-induced cell death in WT, but not in *Sirt1−/−*, mESCs**
(A) Effects of 3-MA and Z-VAD-FMK on R1 (WT) and *Sirt1−/−* (KO) mESCs treated with
1mM $H_2O_2$. Cells were seeded at $2 \times 10^5$ cells/well in 6-well flat-bottomed plates and
incubated overnight at 37 C°. After exposure to 1mM $H_2O_2$ and/or 10 mM autophagy-
specific inhibitor 3-MA or 25μM pan-caspase inhibitor Z-VAD-FMK for 4 hours, cell
viability was measured by apoptosis detection assay. Error bars indicate SDs from the
average of 3 independent experiments, each performed in triplicate. *P<0.05 and
***P<0.001 signifies the main effect of pre-treatment compared groups as indicated in the

corresponding ANOVA. (B) Caspase 3 activity-based cytotoxic assay of WT and *Sirt1−/−* cells treated with 1mM $H_2O_2$ and/or 10 mM 3-MA. Shown is the average of 3 independent experiments, each performed in triplicate. Data are shown as mean ± SD. *P<0.05 and ***P<0.001 signifies the main effect of pre-treatment compared groups as indicated in the corresponding ANOVA. (C) Apoptosis of WT and *Sirt1−/−* mESCs treated with 0.6 mM $H_2O_2$. Cells were stained with PI and Annexin-V–FITC, and the positive stained cells were counted using FACScan. Representative results of one of three independent experiments are shown.
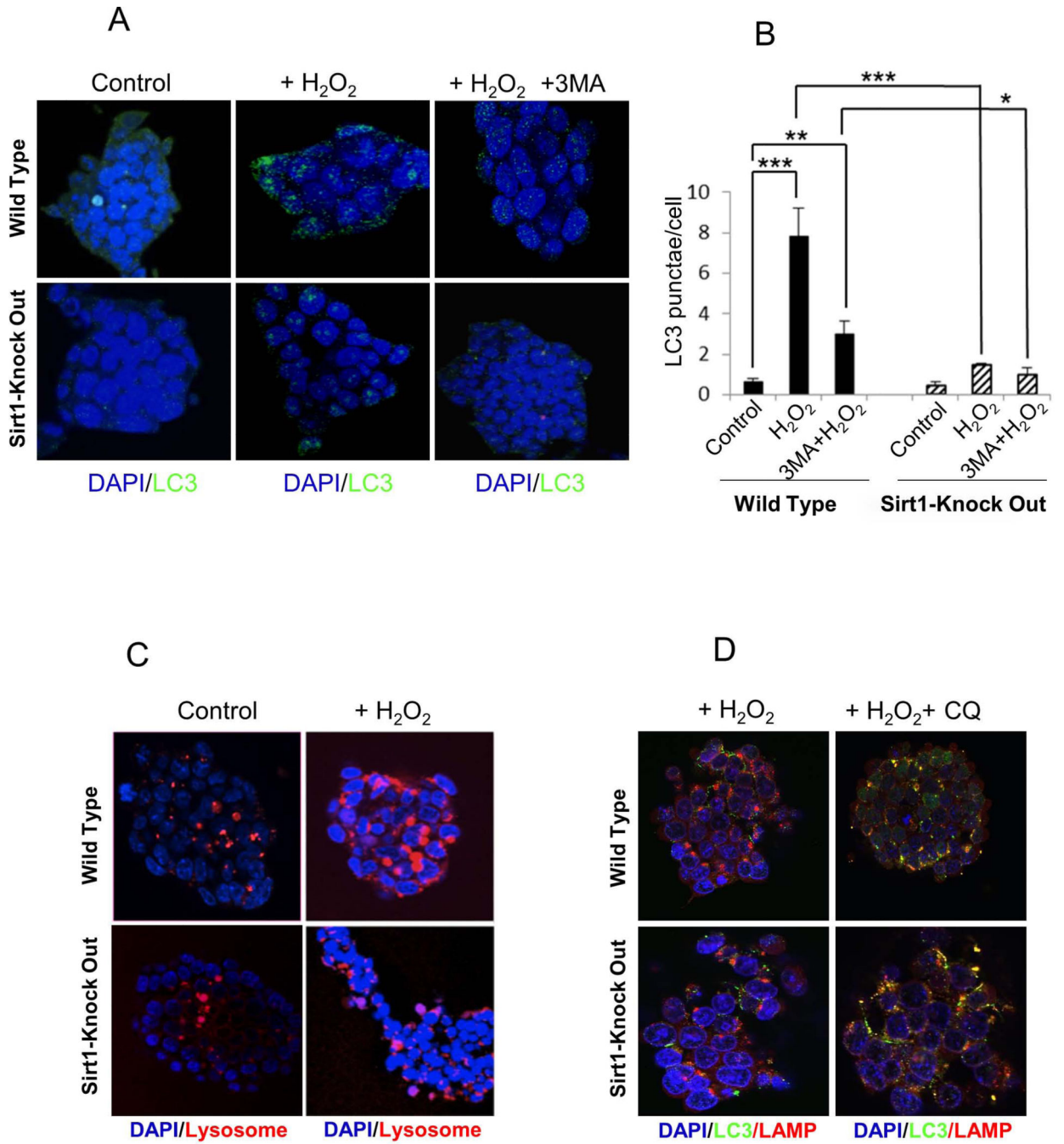
**Fig 2. 1mM H$_2$O$_2$ induces less autophagy in *Sirt1−/−*, compared to WT, mESCs**
(A) Fluorescence microscopic images of LC3 in WT and *Sirt1−/−* (KO) mESCs after
treatment with 1mM H$_2$O$_2$ and/or 10 mM 3-MA for 4 hours. Green fluorescence indicates
LC3. Nuclei were counterstained with DAPI (blue). (B) Quantification of LC3 punctae in
WT and *Sirt1−/−* cells after treatment with 1mM H$_2$O$_2$ and/or 10 mM 3-MA for 4 hours.
Results are the average of 3 independent experiments, each performed in triplicate. Data are
shown as mean ± SD. *P<0.05, **P<0.01, and ***P<0.001 signifies the main effect of pre-
treatment compared groups as indicated in the corresponding ANOVA. (C) LysoTracker-

stained confocal microscopic images of WT and *Sirt1−/−* cells 30 min after exposure to control medium or 1mM $H_2O_2$. Red fluorescence indicates lysosome. Nuclei were counterstained with DAPI (blue). (D) Double-immunocytochemical staining of WT and *Sirt1−/−* cells with anti-LC3 and anti-LAMP-1 antibodies. Cells were treated with 1mM $H_2O_2$ with/without 50 μM Chloroquine (CQ) for 30 min. LC3 expression represents green and LAMP-1 represents red fluorescence. Fusion between autophagosomes and lysosomes was evident in both cell lines.

A

Wild Type

Sirt1-Knock Out

B

C

WT Control · WT+3MA · WT+H₂O₂ · WT+H₂O₂+3MA

KO Control · KO+3MA · KO+H₂O₂ · KO+H₂O₂+3MA

JC-1 red fluorescence

JC-1 green fluorescence

D

E
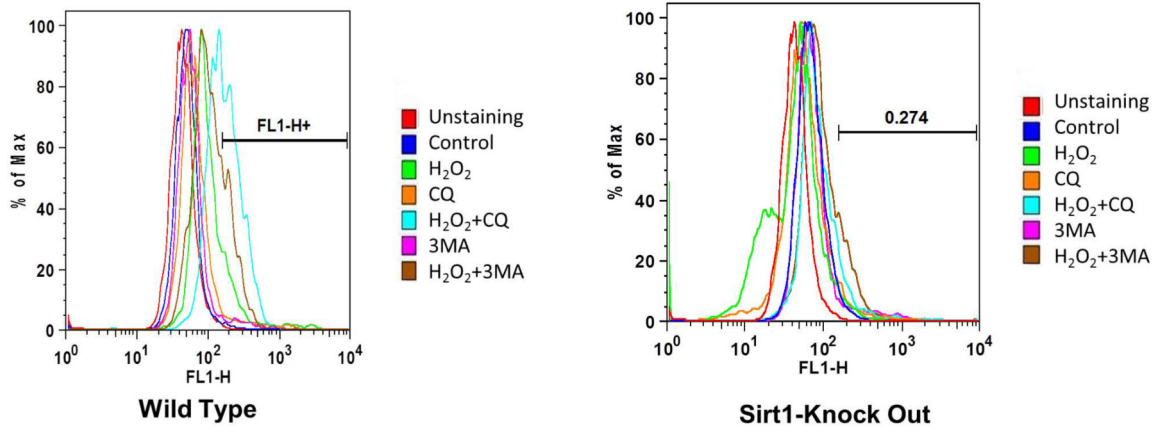
**Fig 3. SIRT1 is necessary for autophagy and associated mitochondrial dynamics**
(A) Histograms for intracellular ROS levels in WT and *Sirt1−/−* mESCs treated with 1mM
$H_2O_2$ and/or 10mM 3-MA and/or 50 μM Chloroquine (CQ) for 4 hours. Cells were stained
with DCF-DA and the fluorescence was measured with FACScan. (B) Quantification of
intracellular ROS levels in WT and *Sirt1−/−* mESCs treated with 1mM $H_2O_2$ and/or 10mM
3-MA and/or 50 μM CQ for 4 hours. Shown are results of the average of 3 independent
experiments, each performed in triplicate. Data are shown as mean ± SD. **$P<0.01$ and
***$P<0.001$ signifies the main effect of pre-treatment compared groups as indicated in the
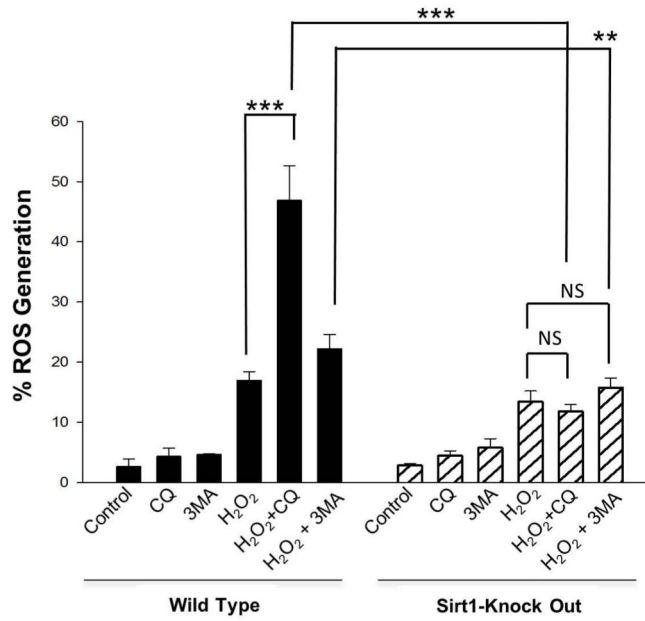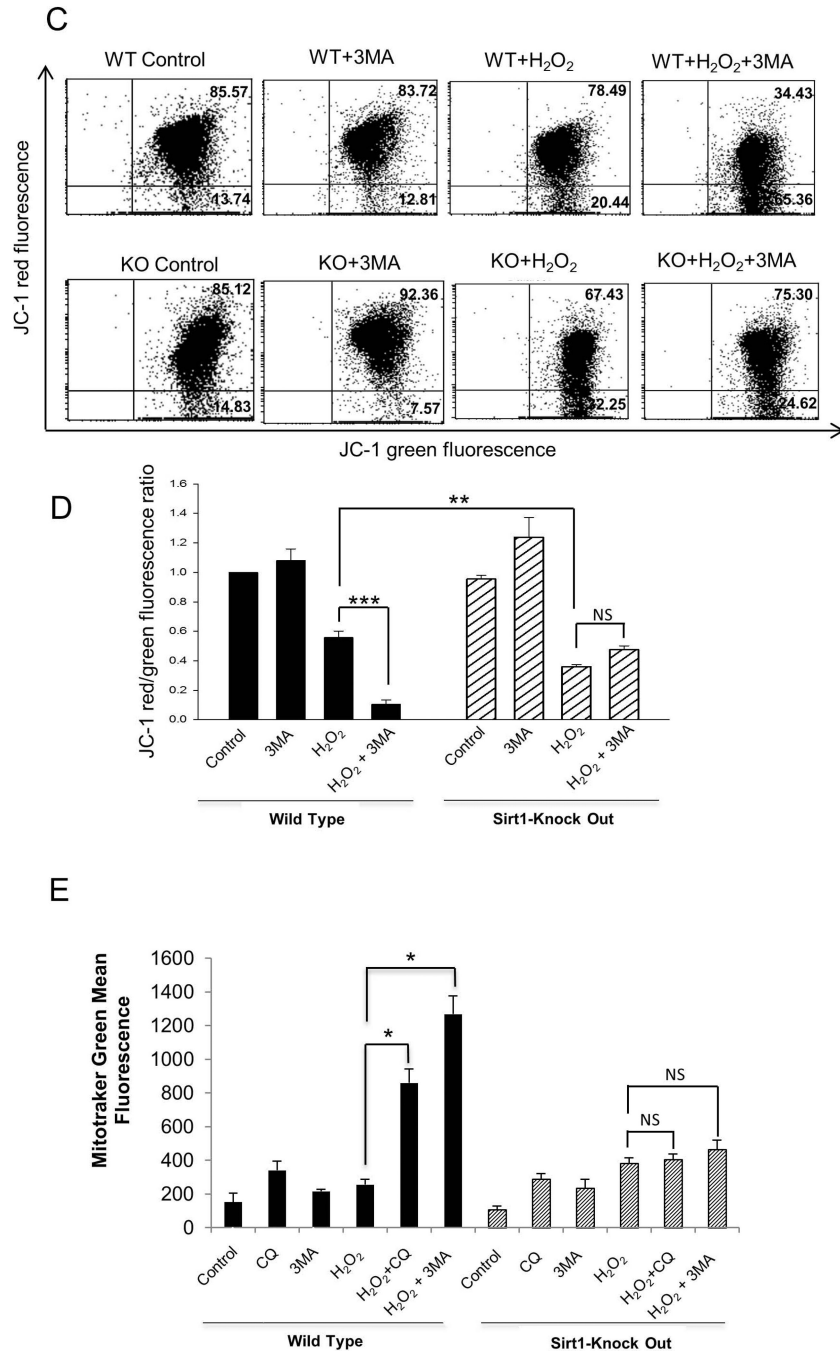
corresponding ANOVA. (C) Flow cytometry analysis of JC-1, a probe that measures mitochondrial membrane potential, in WT and *Sirt1−/−* mESCs treated with 1mM $H_2O_2$ and/or 10mM 3-MA. (D) Quantitative and statistical analysis comparing mitochondrial membrane potential by JC-1 staining in in WT and *Sirt1−/−* mESCs treated with 1mM $H_2O_2$ and/or 10mM 3-MA. The average of 3 independent experiments, each performed in triplicate are shown. Data are shown as mean ± SD. **P<0.01 and ***P<0.001 signifies the main effect of pre-treatment compared groups as indicated in the corresponding ANOVA. (E) Quantitative comparison of average mitotracker green staining in WT and *Sirt1−/−* mESCs treated with 1mM $H_2O_2$ and/or 10mM 3-MA and/or 50 μM CQ for 4 hours. Results are shown as the average of 3 independent experiments, each performed in triplicate. Data are shown as mean ± SD. *P<0.05 signifies the main effect of pre-treatment compared groups.
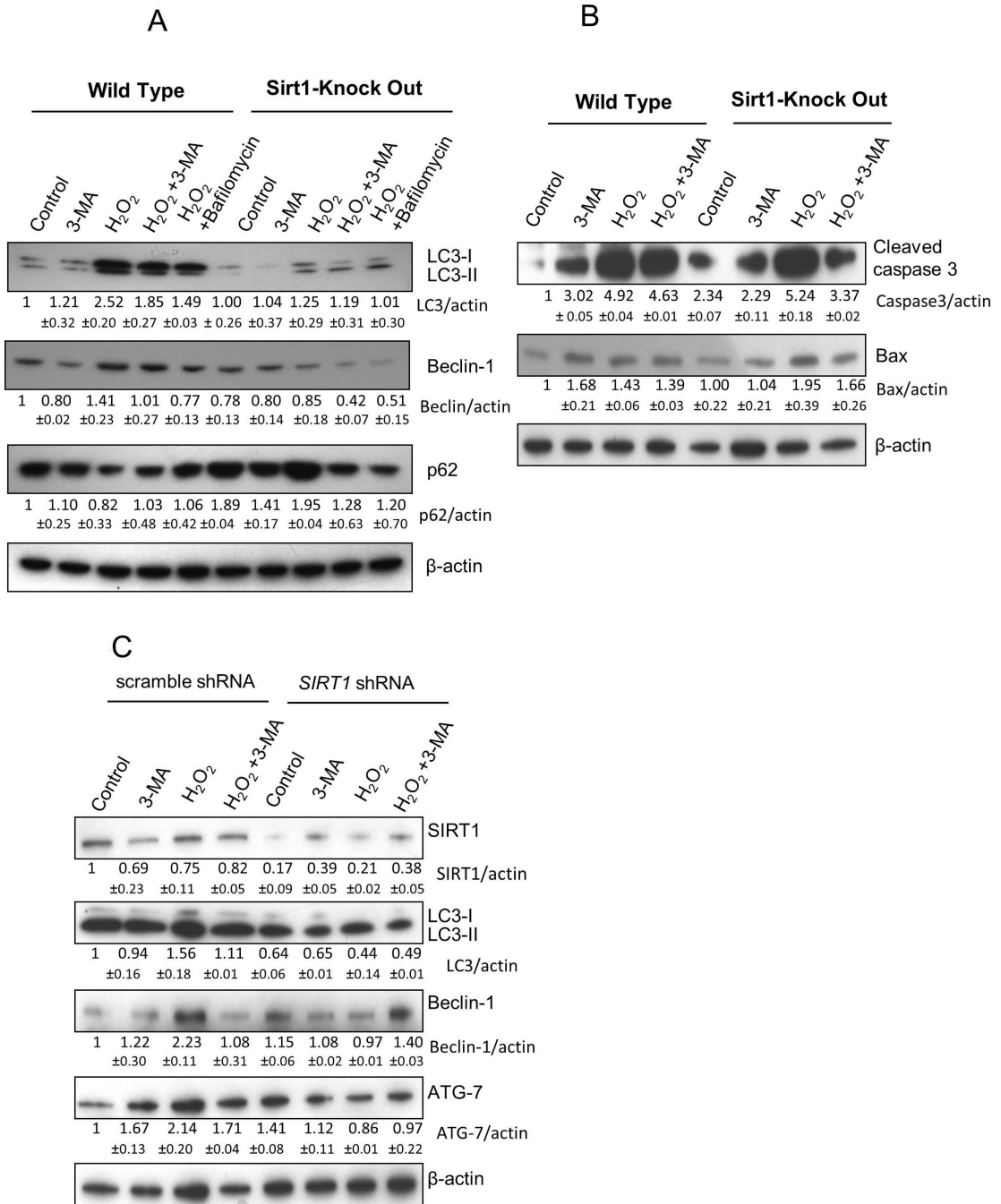
**Fig 4. H$_2$O$_2$ increases levels of autophagy markers in WT compared to *Sirt1−/−* ESCs**
(A) H$_2$O$_2$ upregulates conversion of LC3-I to LC3-II and Beclin-1, both of which are the markers for autophagy, in WT, compared to *Sirt1−/−*, cells. Addition of 3-MA and bafilomycin inhibits LC3 cleavage and Beclin-1 expression induced by H$_2$O$_2$ in WT cells but not in *Sirt1−/−* cells. Data represent one of three independent experiments with similar results. (B) H$_2$O$_2$ induces apoptosis similarly in both cell lines as evaluated by the activation of cleaved caspase 3 and expressions of Bax. Data shown represent one of three independent experiments that gave similar results. (C) Knock-down of *SIRT1* expression by Lentivirus

shRNA in hESCs showed decreased conversion of LC3-I to LC3-II, Beclin 1, and ATG7 expression compared to hESCs transduced with scrambled shRNA after cells were treated with 0.1mM $H_2O_2$ and/or 10 mM 3-MA. Data represent one of three independent experiments that gave similar results. In order to provide the quantification for all of bands, we measured them using Image-J. The values under the bands represent the ratio of band intensity for target protein to band intensity for housekeeping gene actin. Underneath each blot, relative expression levels mean values of each protein as fold induction for target protein to band intensity for housekeeping gene actin protein above expression levels in nontreated control cells. Data are shown as mean ± SD.

## A

Wild Type    Sirt1-Knock Out

Control    3-MA    H$_2$O$_2$    H$_2$O$_2$ +3-MA    Control    3-MA    H$_2$O$_2$    H$_2$O$_2$ +3-MA

p-P70/S6K (T389)

| 1 | 1.66 | 0.83 | 2.37 | 1.20 | 1.68 | 1.94 | 1.34 | P-P70/P70 |
|---|---|---|---|---|---|---|---|---|
| | ±0.17 | ±0.18 | ±0.28 | ±0.29 | ±0.27 | ±0.11 | ±0.24 | |

P70/S6K

ribosomal p-S6

| 1 | 1.33 | 0.69 | 2.03 | 1.79 | 1.90 | 1.84 | 1.77 | P-S6 R/S6 R |
|---|---|---|---|---|---|---|---|---|
| | ±0.24 | ±0.14 | ±0.45 | ±0.37 | ±0.38 | ±0.25 | ±0.22 | |

ribosomal S6

β-actin

## B

scramble shRNA    SIRT1 shRNA

Control    3-MA    H$_2$O$_2$    H$_2$O$_2$ +3-MA    Control    3-MA    H$_2$O$_2$    H$_2$O$_2$ +3-MA

p-P70/85 S6K (T389)

| 1 | 1.25 | 0.86 | 1.66 | 1.22 | 1.32 | 1.76 | 1.37 | P-P70/P70 |
|---|---|---|---|---|---|---|---|---|
| | ±0.21 | ±0.02 | ±0.39 | ±0.23 | ±0.12 | ±0.18 | ±0.11 | |

P70/85 S6K

ribosomal p-S6

| 1 | 1.12 | 0.65 | 1.93 | 0.89 | 0.87 | 2.28 | 1.09 | P-S6 R/S6 R |
|---|---|---|---|---|---|---|---|---|
| | ±0.67 | ±0.55 | ±0.41 | ±0.55 | ±0.48 | ±0.42 | ±0.39 | |

ribosomal S6

β-actin

## C

SIRT1-/- +SIRT1    SIRT1-/- +null

Control    3-MA    H$_2$O$_2$    H$_2$O$_2$ +3-MA    Control    3-MA    H$_2$O$_2$    H$_2$O$_2$ +3-MA

LC3-I
LC3-II

| 1 | 0.84 | 1.46 | 1.55 | 1.55 | 1.62 | 0.19 | 0.41 | LC3/actin |
|---|---|---|---|---|---|---|---|---|
| | ±0.02 | ±0.09 | ±0.10 | ±0.04 | ±0.33 | ±0.03 | ±0.03 | |

Beclin-1

| 1 | 0.88 | 0.85 | 0.77 | 1.02 | 1.21 | 0.26 | 0.33 | Beclin-1/actin |
|---|---|---|---|---|---|---|---|---|
| | ±0.09 | ±0.13 | ±0.05 | ±0.07 | ±0.06 | ±0.01 | ±0.03 | |

β-actin

**Fig 5. SIRT1 regulates autophagy in ESCs through inhibition of the mTOR pathway**
(A) WT and *Sirt1 −/−* mESCs were treated with 1mM H$_2$O$_2$ and/or 10 mM 3-MA. Lysates from cells were analyzed by SDS-PAGE. Protein levels and phosphorylation status of p70/85 S6 kinase and ribosomal S6 were visualized by immunoblotting using specific antibodies. Data represent one of three independent experiments that gave similar results. (B) Knock-down of *SIRT1* expression in hESCs by Lentivirus shRNA showed increased phosphorylation of p70/85 S6 kinase and S6 compared to hESCs transduced with scrambled shRNA after cells were treated with 0.1mM H$_2$O$_2$ and/or 10mM 3-MA. Data represent one

of three independent experiments with similar results. (C) *Sirt1−/−* mESCs reconstituted with WT *Sirt1* gene and *Sirt1−/−* mESCs transduced with vector containing EGFP gene alone were treated with 1mM $H_2O_2$ and/or 10mM 3-MA. Lysates from cells were analyzed by SDS-PAGE. Protein levels of LC3 and Beclin-1 were visualized by immunoblotting using specific antibodies. Data shown represent one of three independent experiments with similar results. Relative expression levels compare to beta-actin controls are given under the bands. Underneath each blot, relative expression levels mean values of each protein as fold induction for target protein to band intensity for housekeeping gene actin protein above expression levels in nontreated control cells. Data are shown as mean ± SD.